Glycoconj J (2009) 26:975–986
DOI 10.1007/s10719-008-9146-4

Structural characterisation of neutrophil glycans by ultra sensitive mass spectrometric glycomics methodology

Ponnusamy Babu · Simon J. North · Jihye Jang-Lee · Sara Chalabi · Kathryn Mackerness · Sean R. Stowell · Richard D. Cummings · Sara Rankin · Anne Dell · Stuart M. Haslam

Received: 11 April 2008 / Revised: 13 May 2008 / Accepted: 15 May 2008 / Published online: 28 June 2008

Abstract Neutrophils are the most abundant white blood cells in humans and play a vital role in several aspects of the immune response. Numerous reports have implicated neutrophil glycosylation as an important factor in mediating these interactions. We report here the application of high sensitivity glycomics methodologies, including matrix assisted laser desorption ionisation (MALDI-TOF) and MALDI-TOF/TOF analyses, to the structural analysis of *N*- and *O*-linked carbohydrates released from two samples of neutrophils, prepared by two separate and geographically remote laboratories. The data produced demonstrates that the cells display a diverse range of sialylated and fucosylated complex glycans, with a high level of similarity between the two preparations.

Keywords Mass spectrometry · Neutrophil · Glycomics · Protein glycosylation

Abbreviations

PNGase F	Peptide *N*-glycosidase F
MALDI	Matrix assisted laser desorption ionisation
CAD	Collision activated decomposition
Hex	Hexose
HexNAc	*N*-acetylhexosamine
ESL-1	E-selectin ligand-1
FAB	Fast atom bombardment
Fuc	Fucose
Gal	Galactose
GalNAc	*N*-acetylgalactosamine
Glc	Glucose
GlcNAc	*N*-acetylglucosamine
Man	Mannose
NeuAc	*N*-acetylneuraminic acid
MS	Mass spectrometry
MS/MS	Tandem mass spectrometry
PSGL-1	P-selectin glycoprotein ligand 1
TOF	Time of flight
Le^x	$Lewis^x$
Le^a	$Lewis^a$
sLe^x	Sialyl $Lewis^x$
sLe^a	Sialyl $Lewis^a$

P. Babu · S. J. North · J. Jang-Lee · S. Chalabi · A. Dell · S. M. Haslam (✉)
Division of Molecular Biosciences,
Faculty of Natural Sciences, Imperial College London,
London SW7 2AZ, UK
e-mail: s.haslam@imperial.ac.uk

K. Mackerness · S. Rankin
Department of Leukocyte Biology, National Heart and Lung Institute, Faculty of Medicine, Imperial College London,
London SW7 2AZ, UK

S. R. Stowell · R. D. Cummings
School of Medicine, Biochemistry, Emory University,
201 Dowman Drive,
Atlanta, GA 30322, USA

Introduction

Neutrophils are the most abundant white blood cells in humans. During an acute inflammatory response, circulating neutrophils interact with the activated endothelium through receptor-mediated processes involving selectins and integrins. Neutrophils interact with P-selectin, E-selectin and other adhesion molecules on activated endothelial cells or captured platelets to initiate leukocyte rolling and tethering [1–3]. This promotes leukocyte activation and integrin-mediated adhesion that allows activated neutrophils to migrate from the circulation into the tissue space. Neutrophils are the first

immune cells to react to inflammation or infection via chemotaxis, internalising and killing microorganisms and ingesting particles through the process of phagocytosis. Defects in phagocytosis can lead to immunodeficiency related diseases in children [4]. Decreased neutrophil adherence and impaired chemotaxis have also been associated with congenital recurrence infections [5–7]. The tethering of neutrophils is mediated by cell surface carbohydrate ligands and selectins present on the endothelial cells [8]. The structural characterization of cell surface glycoconjugates from neutrophil granulocytes was first addressed more than two decades ago using Fast Atom Bombardment mass spectrometry (FAB-MS) complemented by linkage analyses and exoglycosidase digests [9]. This technology showed that the cell surface N-glycans were highly fucosylated and sialylated and many of their antenna were comprised of poly-*N*-acetyllactosaminyl backbones (-3Galβ1-4GlcNAcβ1-)$_n$, often referred to as polyLacNAc. Also identified was the sialyl Lewis^x epitope (NeuAcα2–3Galβ1(Fucα1–3)4GlcNAc-R) which, several years later, was shown to play a critical role in selectin-mediated neutrophil trafficking [10–14].

FAB-MS technology was a powerful technique for defining the structures of glycan determinants at the non-reducing ends of the N-glycan antennae and for giving an indication of the length of antennae. This information was afforded by A-type fragment ions that were produced in the source of the FAB mass spectrometer via cleavage at each of the GlcNAc residues during the ionisation of permethylated glycans [15]. The weakness of the FAB-MS experiment was its poor sensitivity above *m/z* 3000 and the high chemical noise background throughout the observable mass range which made detection of minor components very difficult. Thus, although the FAB-MS experiments of the 1980s revealed vitally important aspects of neutrophil glycosylation, their characterisation of the neutrophil glycome was far from comprehensive.

Recent advancements in mass spectrometric techniques have had an enormous impact on the structural analysis of complex glycan mixtures from cells and tissues and it is therefore timely to reassess neutrophil glycosylation [16]. Probably the most significant mass spectrometric advance has been the replacement of FAB-MS instrumentation by MALDI-TOF and MALDI-TOF/TOF-MS. This has enabled very significant increases in levels of sensitivity, upper mass range and reduced levels of chemical noise background. Most significantly the tandem MS/MS capability of MALDI-TOF/TOF instrumentation means that individual glycan molecular ions, even at high *m/z* values, can be fragmented to afford structurally informative fragment ion data [17]. However a critical step still remains the permethylation of glycans as this not only increases the sensitivity of the analysis but also facilitates the unambiguous sequencing of individual carbohydrate structures in MS/MS experiments.

In this paper we document the structural analysis of N- and O-glycans from resting human neutrophils using the above described strategy. To establish sample-sample consistency, two batches of cells were prepared by geographically remote groups, one based in the UK and one in the US. Permethylated N-glycans up to *m/z* 6500 in mass were detected in derivatised PNGase F released material, the largest intact N-glycans thus far directly observed by MS in human samples. The sialyl Le^x containing carbohydrate cell surface antigens present on the neutrophils were characterized by high-sensitivity MS/MS techniques. We found that sialyl Le^x containing glycans constitute less than 0.05% of the total N-glycans observed, while approximately 5% of the O-glycan structures contain sialyl Le^x as a terminal epitope. In addition, the robust and reproducible nature of the glycomic methodologies employed is highlighted by the fact that variation between Sample 1 (US) and Sample 2 (UK) was minimal.

Materials and methods

Materials

All the reagents used in this study were of high purity obtained from Sigma-Aldrich except as noted.

Mixed granulocyte preparation and isolation of neutrophils

Human neutrophils sample 1 (USA) were isolated in accordance with a protocol approved by the OUHSC Institutional Review Board. Neutrophils were isolated by drawing 30 ml whole blood into a 60 ml syringe containing 100 U heparin, mixed with a 6% Dextran 70 in 0.9% Sodium Chloride injection USP (Braun Medical Inc.) and allowed to sediment for 30 min at RT. The leukocyte fraction was then isolated, centrifuged and subjected to hypotonic lysis to remove contaminating RBCs. Leukocytes were then subjected to density gradient centrifugation using Histopague-1077 (Sigma-Aldrich) followed by washing cells twice in HBSS using the procedure of Zimmerman *et al.* 1985, [18]. Isolated cells were found to be >90% neutrophils by Wright–Giemsa staining.

The isolation of human neutrophils from Sample 2 (UK) was carried out according to a protocol approved by St. Mary's Hospital (London, UK). Neutrophils were isolated by drawing 30 ml whole blood into a 60 ml syringe containing 4.4 ml of 3.8% trisodium citrate (Citric Acid Sigma Cat. No. C8532). The blood was centrifuged at 310 g for 20 min (no brake applied) and the top layer of

platelet-rich plasma was discarded. The remaining erythrocytes and buffy coat were mixed with a 6% Dextran® (GE Healthcare Cat. No. 17-0320-01) and 0.9% sterile Sodium Chloride was added up to 50 ml and allowed to sediment for 20 min at RT. The leukocyte fraction was then subjected to density gradient centrifugation using Histopague-1077 (Sigma-Aldrich). The remaining erythrocytes were lysed by hypotonic lysis. Neutrophils were positively isolated from the mixed granulocyte preparation using anti-CD16 microbeads (50 μl of beads per 50×106 cells, Miltenyi Biotec Cat. No. 130-045-701) and Miltenyi LS columns. This yielded neutrophils of 99% purity [19].

Reduction and carboxymethylation

Approximately 2×10^7 human neutrophil cells were sonicated in extraction buffer (25 mM Tris, 150 mM NaCl, 5 mM EDTA and 1% CHAPS at pH 7.4) and then dialysed against 4×4.5 l of 50 mM ammonium bicarbonate, pH 8.5, at 4°C for 48 h (as described previously [20]). After dialysis, the sample was lyophilized. The sample was then reduced in 1 ml of 50 mM Tris–HCl buffer, pH 8.5, containing 2 mg/ml dithiothreitol. Reduction was performed under a nitrogen atmosphere at 37°C for 1 h. Carboxymethylation was carried out by the addition of iodoacetic acid (five-fold molar excess over dithiothreitol), and the reaction was allowed to proceed under a nitrogen atmosphere at room temperature in the dark for 2 h. Carboxymethylation was terminated by dialysis against 4×4.5 l of 50 mM ammonium bicarbonate, pH 8.5, at 4°C for 48 h. After dialysis, the sample was lyophilized.

Tryptic digest

The reduced carboxymethylated proteins were digested with TPCK pre-treated bovine pancreas trypsin (EC 3.4.21.4, Sigma), for 16 h at 37°C in 50 mM ammonium bicarbonate buffer (pH 8.4). The products were purified by C18-Sep-Pak (Waters Corp.) as described [21].

Sep-Pak® separation of released glycans from peptides

The reverse-phase C_{18} Sep-Pak cartridge was primed sequentially with 5 ml methanol, 5 ml 5% acetic acid (v/v) and 5 ml propan-1-ol before being re-equilibrated with 10 ml 5% acetic acid (v/v). The sample was then dissolved in a minimum volume of 5% acetic acid (v/v) and loaded directly onto the Sep-Pak. Elution was achieved using 3 ml of 5% acetic acid (v/v), followed by 2 ml each of 20%, 40%, 60% and 100% propan-1-ol in 5% acetic acid (v/v). Each elution step was collected, reduced in volume on a Speed Vac and lyophilised [21].

PNGase F digestion of glycopeptides

PNGase F (EC3.5.1.52, Roche Molecular Biochemicals, Lewes, UK) digestion was carried out in 200 μl ammonium bicarbonate (50 mM, pH 8.5) for 16 h at 37°C using 3 U of enzyme. The reaction was terminated by lyophilization and the released N-glycans were separated from peptides and O-glycopeptides by Sep-Pak C18 (Waters, Elstree, UK) as described [22].

Sep-Pak® separation of permethylated glycans

The reverse-phase C_{18} Sep-Pak cartridge was primed sequentially with 5 ml methanol, 5 ml water and 5 ml acetonitrile before being re-equilibrated with 10 ml of water. The lyophilised permethylated oligosaccharide sample was then dissolved in a minimum volume of methanol and loaded directly onto the Sep-Pak. Elution was achieved using 3 ml of water followed by 2 ml each of 15%, 30%, 50%, 75% and 100% acetonitrile in water (v/v). Each elution step was collected, reduced in volume on a Speed Vac and lyophilised [22].

Reductive elimination

O-glycans were released by reductive elimination in 400 μL of 0.1 M potassium borohydride (54 mg/ml of potassium hydroxide in water) solution at 45°C for 16 h. The reaction was terminated by dropwise addition of glacial acetic acid, followed by Dowex 50W-X8 (H) 50–100 mesh (Sigma) chromatography and borate removal.

Neuraminidase treatment

A portion of the underivatised N-glycan was dissolved in 100 μl pH 5.5 50 mM ammonium acetate buffer and incubated at 37°C with 50 U of *Vibrio cholerae* neuraminidase (EC No. 3.2.1.18). After 18 h the sample was lyophilized and then permethylated before MALDI-TOF analysis.

Derivatisation for MALDI-TOF and tandem mass spectrometry analysis

Permethylation was performed using the sodium hydroxide procedure, as described previously [22]. 1 g of sodium hydroxide pellets were crushed in a glass mortar with 3 ml distilled, anhydrous DMSO. 1 ml of the resulting slurry and 200 μl of methyl iodide were added to the lyophilised sample. The mixture was then shaken for 10 min before the reaction was quenched by dropwise addition of water. The permethylated sample was then extracted into 1 ml of chloroform and washed with 4×1 ml of water. The chloroform was then removed under a stream of nitrogen.

Mass spectrometric analysis

MALDI-TOF data were acquired on a Voyager-DE STR mass spectrometer (Applied Biosystems, Foster City, CA) in the reflectron mode with delayed extraction. Permethylated samples were dissolved in 10 μl of methanol and 1 μl of dissolved sample was premixed with 1 μl of matrix (20 mg/ml 2,5-dihydroxybenzoic acid (DHB) in 70% (v/v) aqueous methanol), spotted onto a target plate and dried under vacuum.

Peaks observed in the MS spectra were selected for further MS/MS. MS/MS data were acquired using a 4800 MALDI TOF/TOF (Applied Biosystems) mass spectrometer. The potential difference between the source acceleration voltage and the collision cell was set to 1 kV and argon was used as collision gas. The 4700 Calibration Standard kit, calmix (Applied Biosystems), was used as the external calibrant for the MS mode and [Glu1] fibrinopeptide B human (Sigma-Aldrich) was used as an external calibrant for the MS/MS mode.

Automated MS and MS/MS analysis

Annotation of the MS and MS/MS data was achieved with assistance from the Cartoonist algorithm [23] and the GlycoWorkbench software suite [24].

Results

Employed strategy

In this communication we report the N- and O-glycan profiles from human neutrophils using mass spectrometry. Cell preparations from the Cummings (Sample 1 (US)) and the Rankin (Sample 2 (UK)) laboratories were sonicated, reduced/carboxymethylated and digested with trypsin. The preparation of tryptic glycopeptides facilitates the release of N- and O-glycans by PNGase F and reductive elimination, respectively. Purified glycans were permethylated to enhance the sensitivity of detection and to direct the subsequent MS/MS fragmentation.

MALDI-MS was employed to obtain a profile of the molecular ions giving singly charged sodiated molecular ions $[M+Na]^+$. Although not fully quantitative, recent studies have demonstrated that relative quantitation based on signal intensities of permethylated glycans analyzed by MALDI-TOF MS is a reliable method, especially when comparing signals over a small mass range within the same spectrum [17]. Molecular ions observed in the MS spectrum were subjected to MS/MS analysis, which afforded sequence informative fragment ions that provided vital structural information such as the non-reducing end sequences *i.e.* antennae structures, branching patterns and sometimes linkage positions. The assignments of neutrophil N-glycan spectra were carried out with the assistance of Cartoonist [23], a bespoke algorithm designed to mimic the human approach to the analysis and assignment of N-glycan MALDI spectra. Cartoonist searches the raw MS data for peak envelopes and uses knowledge of the biosynthetic pathways in order to present the user with the most likely permethylated carbohydrate structures for each signal. MS/MS spectra were assigned with the support of the GlycoWorkbench suite [24] of software tools, which are designed to assist the experts during the annotation of glycan fragment spectra. The graphical interface of GlycoWorkbench provides an environment in which structure models can be rapidly assembled, automatically matched with MS^n data and compared to assess the best candidate.

MALDI-TOF analysis of released N-glycans from human neutrophils

Samples of human neutrophil cells from the two geographically remote sources (see "Materials and methods") were subjected to glycan profiling by MALDI-TOF MS analysis. The mass spectra of the PNGase F released glycans (Fig. 1 and Table 1) were exceptionally rich in molecular ion signals, corresponding to $[M+Na]^+$ adducts up to *m/z* 6500. A relatively small amount of the sample (less than 5%) was represented by the high mannose type structures (observed at *m/z* 1580.2, 1784.2, 1988.2, 2192.2 and 2396.1), with the vast majority of observed signals being consistent with complex type glycans, comprising of bi-, tri-, and tetra-antennary structures, capped with one, two, three or four sialic acid residues. There was a high degree of fucosylation amongst the complex glycans, with structures consistent with both $Le^{x/a}$ and sialyl $Le^{x/a}$ antennae, as well as prevalent polyLacNAc extensions (*m/z* 2401.1–6528.1, Table 1). Previous detailed evidence from our neutrophil studies categorically established that the antennae are Le^x and sialyl Le^x rather than Le^a and sialyl Le^a [9].

MALDI-TOF/TOF analysis of released N-glycans from human neutrophils

Collision-activated decomposition (CAD) MALDI-TOF/TOF MS/MS experiments were carried out upon molecular ions observed in the MALDI spectrum, yielding fragment ions that defined structural features including core fucosylation, antennal LacNAc extensions, Le^x and sialyl Le^x epitopes. These experiments were carried out on both neutrophil samples, and returned highly consistent results. Data representative of these experiments is shown in Fig. 2 (*m/z* 3141.1 and *m/z* 3766.6).

The most prominent peak in each sample is that of a bi-antennary, mono-sialylated, di-fucosylated structure of the

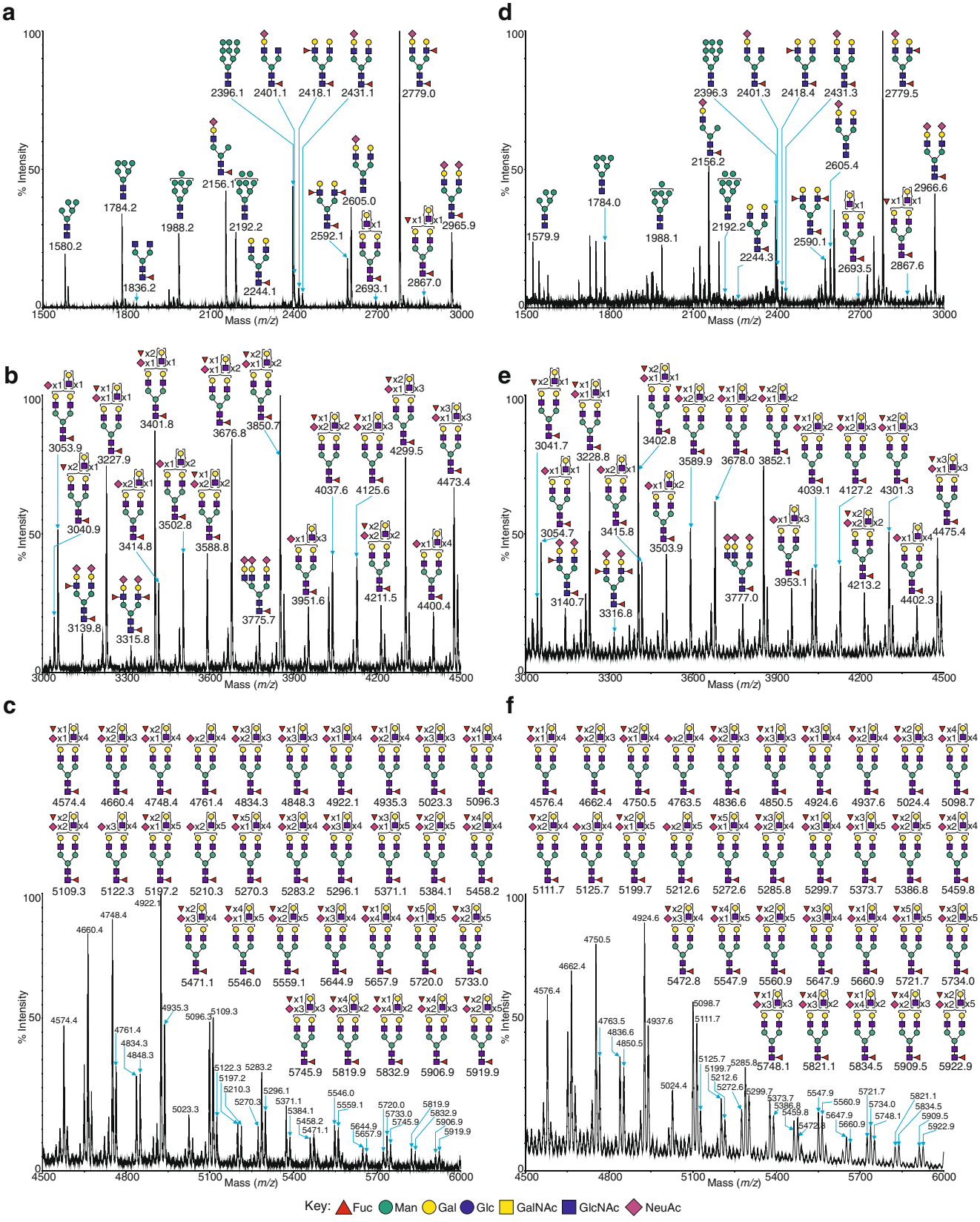

Fig. 1 MALDI-TOF MS profiles of the permethylated N-linked glycans from human neutrophils. Major peaks are annotated with the relevant carbohydrate structure shown in symbol form, according to the glycan nomenclature adopted by the CFG (http://www.functionalglycomics.org/). Neutrophil Sample 1 (US) is displayed in panels (a), (b) and (c). Neutrophil Sample 2 (UK) is displayed in panels (d), (e) and (f). For complete annotation of the spectra see Table 1. All molecular ions are present in sodiated form ($[M+Na]^+$)

Table 1 Compositional assignments of singly charged sodiated molecular ions, $[M+Na]^+$, observed in MALDI-MS spectra of permethylated N-glycans from human neutrophils

Signal (*m/z*) Sample 1 (US)	Signal (*m/z*) Sample 2 (UK)	Molecular Assignments
1580.2	1579.9	$Hex_5HexNAc_2$
1591.2	1591.0	$Fuc_1Hex_3HexNAc_3$
1765.2	1765.0	$Fuc_2Hex_3HexNAc_3$
1784.2	1784.0	$Hex_6HexNAc_2$
1795.2	1795.0	$Fuc_1Hex_4HexNAc_3$
1836.2	–	$Fuc_1Hex_3HexNAc_4$
1952.2	1952.1	$NeuAc_1Fuc_1Hex_3HexNAc_3$
1969.2	1969.1	$Fuc_2Hex_4HexNAc_3$
1988.2	1988.1	$Hex_7HexNAc_2$
2040.1	2040.2	$Fuc_1Hex_4HexNAc_4$
2082.1	2081.1	$Fuc_1Hex_3HexNAc_5$
2156.1	2156.2	$NeuAc_1Fuc_1Hex_4HexNAc_3$
2192.2	2192.2	$Hex_8HexNAc_2$
2244.1	2244.3	$Fuc_1Hex_5HexNAc_4$
2396.1	2396.3	$Hex_9HexNAc_2$
2401.1	2401.3	$NeuAc_1Fuc_1Hex_4HexNAc_4$
2418.1	2418.4	$Fuc_2Hex_5HexNAc_4$
2431.1	2431.3	$NeuAc_1Hex_5HexNAc_4$
2592.1	2592.4	$Fuc_3Hex_5HexNAc_4$
2605.0	2605.4	$NeuAc_1Fuc_1Hex_5HexNAc_4$
2693.1	2693.5	$Fuc_1Hex_6HexNAc_5$
2779.0	2779.5	$NeuAc_1Fuc_2Hex_5HexNAc_4$
2867.0	2867.6	$Fuc_2Hex_6HexNAc_5$
2965.9	2966.6	$NeuAc_2Fuc_1Hex_5HexNAc_4$
3040.9	3041.7	$Fuc_3Hex_6HexNAc_5$
3053.9	3054.7	$NeuAc_1Fuc_1Hex_6HexNAc_5$
3139.8	3140.7	$NeuAc_2Fuc_2Hex_5HexNAc_4$
3227.9	3228.8	$NeuAc_1Fuc_2Hex_6HexNAc_5$
3315.8	3316.8	$Fuc_2Hex_7HexNAc_6$
3401.8	3402.8	$NeuAc_1Fuc_3Hex_6HexNAc_5$
3414.8	3415.8	$NeuAc_2Fuc_1Hex_6HexNAc_5$
3502.8	3503.9	$NeuAc_1Fuc_1Hex_7HexNAc_6$
3588.8	3589.9	$NeuAc_2Fuc_2Hex_6HexNAc_5$
3676.8	3678.0	$NeuAc_1Fuc_2Hex_7HexNAc_6$
3775.7	3777.0	$NeuAc_3Fuc_1Hex_6HexNAc_5$
3850.7	3852.1	$NeuAc_1Fuc_3Hex_7HexNAc_6$
3863.6	3865.0	$NeuAc_2Fuc_1Hex_7HexNAc_6$
3951.6	3953.1	$NeuAc_1Fuc_1Hex_8HexNAc_7$
4024.6	4026.2	$NeuAc_1Fuc_4Hex_7HexNAc_6$
4037.6	4039.1	$NeuAc_2Fuc_2Hex_7HexNAc_6$
4125.6	4127.2	$NeuAc_1Fuc_2Hex_8HexNAc_7$
4211.5	4213.2	$NeuAc_2Fuc_3Hex_7HexNAc_6$
4224.6	4226.2	$NeuAc_3Fuc_1Hex_7HexNAc_6$
4299.5	4301.3	$NeuAc_1Fuc_3Hex_8HexNAc_7$
4312.5	4314.3	$NeuAc_2Fuc_1Hex_8HexNAc_7$
4400.4	4402.3	$NeuAc_1Fuc_1Hex_9HexNAc_8$
4473.4	4475.4	$NeuAc_1Fuc_4Hex_8HexNAc_7$
4486.5	4488.3	$NeuAc_2Fuc_2Hex_8HexNAc_7$
4574.4	4576.4	$NeuAc_1Fuc_2Hex_9HexNAc_8$
4660.4	4662.4	$NeuAc_2Fuc_3Hex_8HexNAc_7$
4674.4	4675.4	$NeuAc_3Fuc_1Hex_8HexNAc_7$
4748.4	4750.5	$NeuAc_1Fuc_3Hex_9HexNAc_8$
4761.4	4763.5	$NeuAc_2Fuc_1Hex_9HexNAc_8$
4834.3	4836.6	$NeuAc_2Fuc_4Hex_8HexNAc_7$
4848.3	4850.5	$NeuAc_1Fuc_1Hex_{10}HexNAc_9$
4922.1	4924.6	$NeuAc_1Fuc_4Hex_9HexNAc_8$
4935.3	4937.6	$NeuAc_2Fuc_2Hex_9HexNAc_8$
5023.3	5024.6	$NeuAc_1Fuc_2Hex_{10}HexNAc_9$
5035.3	–	$NeuAc_4Fuc_1Hex_8HexNAc_7$
5096.3	5098.7	$NeuAc_1Fuc_5Hex_9HexNAc_8$
5109.3	5111.7	$NeuAc_2Fuc_3Hex_9HexNAc_8$
5122.3	5125.7	$NeuAc_3Fuc_1Hex_9HexNAc_8$
5197.2	5199.7	$NeuAc_1Fuc_3Hex_{10}HexNAc_9$
5210.3	5212.6	$NeuAc_2Fuc_1Hex_{10}HexNAc_9$
5270.3	5272.6	$NeuAc_1Fuc_6Hex_9HexNAc_8$
5283.2	5285.8	$NeuAc_2Fuc_4Hex_9HexNAc_8$
5296.1	5299.7	$NeuAc_3Fuc_2Hex_9HexNAc_8$
5371.1	5373.7	$NeuAc_1Fuc_4Hex_{10}HexNAc_9$
5384.1	5386.8	$NeuAc_2Fuc_2Hex_{10}HexNAc_9$
5458.2	5459.8	$NeuAc_2Fuc_5Hex_9HexNAc_8$
5471.1	5472.8	$NeuAc_3Fuc_3Hex_9HexNAc_8$
5484.1	5486.8	$NeuAc_4Fuc_1Hex_9HexNAc_8$
5546.0	5547.9	$NeuAc_1Fuc_5Hex_{10}HexNAc_9$
5559.1	5560.9	$NeuAc_2Fuc_3Hex_{10}HexNAc_9$
5572.1	5573.8	$NeuAc_3Fuc_1Hex_{10}HexNAc_9$
5644.9	5647.9	$NeuAc_3Fuc_4Hex_9HexNAc_8$
5657.9	5660.9	$NeuAc_4Fuc_2Hex_9HexNAc_8$
5720.0	5721.7	$NeuAc_1Fuc_6Hex_{10}HexNAc_9$
5733.0	5734.0	$NeuAc_2Fuc_4Hex_{10}HexNAc_9$
5745.9	5748.1	$NeuAc_3Fuc_2Hex_{10}HexNAc_9$
5819.9	5821.1	$NeuAc_3Fuc_5Hex_9HexNAc_8$
5832.9	5834.5	$NeuAc_4Fuc_3Hex_9HexNAc_8$
5906.9	5909.5	$NeuAc_2Fuc_5Hex_{10}HexNAc_9$
5919.9	5922.9	$NeuAc_3Fuc_3Hex_{10}HexNAc_9$
5993.7	5996.0	$NeuAc_3Fuc_6Hex_9HexNAc_8$
6007.1	–	$NeuAc_4Fuc_4Hex_9HexNAc_8$
6079.9	–	$NeuAc_2Fuc_6Hex_{10}HexNAc_9$
6092.7	–	$NeuAc_3Fuc_4Hex_{10}HexNAc_9$
6107.8	–	$NeuAc_4Fuc_2Hex_{10}HexNAc_9$
6168.8	–	$NeuAc_3Fuc_7Hex_9HexNAc_8$
6181.7	–	$NeuAc_4Fuc_5Hex_9HexNAc_8$
6281.6	–	$NeuAc_4Fuc_3Hex_{10}HexNAc_9$
6354.6	–	$NeuAc_4Fuc_6Hex_9HexNAc_8$
6456.2	–	$NeuAc_4Fuc_4Hex_{10}HexNAc_9$
6528.1	–	$NeuAc_4Fuc_7Hex_9HexNAc_8$

empirical composition $NeuAc_1Fuc_2Hex_5HexNAc_4$ (*m/z* 2779.0). Despite being a potential sialyl Le^x structure, MSMS analysis demonstrates that all detectable isomers represented by the peak in fact carry the antennal fucose on the non-sialylated arm (Fig. 2a). This is a theme that persists through the N- and O-glycan samples, highlighting the apparent paucity of sialyl Le^x amongst the neutrophil glycans. As exemplified by this component, whenever there is an option to sialylate and fucosylate separate antenna rather than place both substituents on a single antenna, the

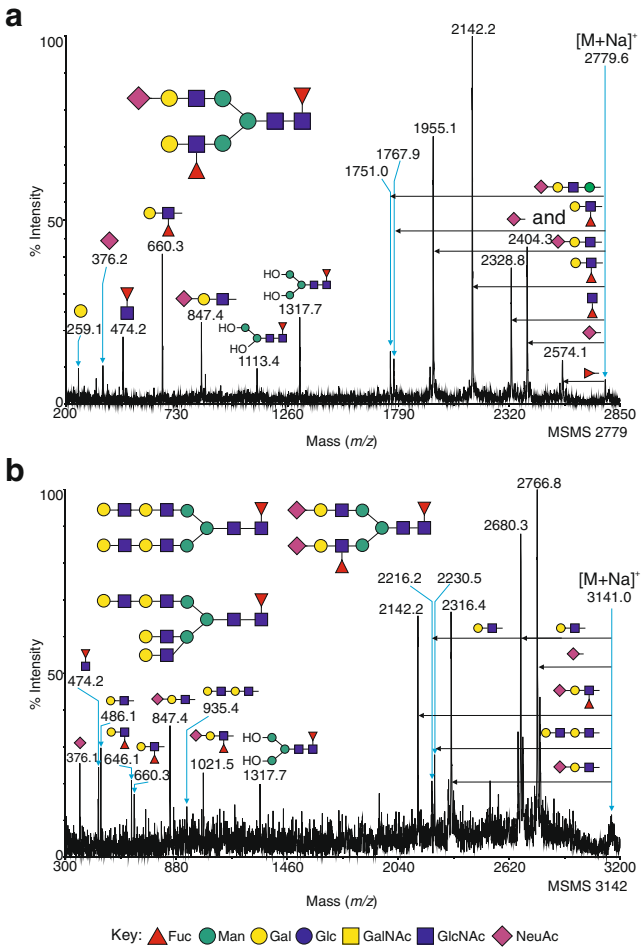

Fig. 2 MALDI-TOF/TOF mass spectrum of the $[M+Na]^+$ molecular ion *m/z* 3766.9 (composition $Fuc_2Hex_8HexNAc_9$, Panel (a)) and *m/z* 3141.0 (compositions $NeuAc_2Fuc_2Hex_5HexNAc_4$ and $Fuc_1Hex_7HexNAc_6$, Panel (b)). Both spectra are derived from the permethylated N-glycans released with PNGase F from neutrophil Sample 2 (UK) (Fig. 1d and e). Assignments of the fragment ions are labelled

former is observed. Thus, despite the composition $NeuAc_1Fuc_2Hex_5HexNAc_4$ being consistent with components carrying a sialyl Le^x antennae, none were observed. Instead the NeuAc is located on an unsubstituted antenna as shown by fragment ions at *m/z* 1751.0, 1955.1 and 847.4, while the fucose residues are present on the chitobiose core (*m/z* 474.1) and on Le^x antennae (*m/z* 660.3, 2142.2 and 1767.9).

The MS/MS analysis of the signals centred at *m/z* 3141.0 (Fig. 2b), initially assigned as $NeuAc_2Fuc_2Hex_5HexNAc_4$, revealed an additional composition, namely $Fuc_1Hex_7HexNAc_6$ which is only two mass units heavier than $NeuAc_2Fuc_2Hex_5HexNAc_4$ and therefore the isotopic clusters overlap. The base peak of the spectrum at *m/z* 2766.8 represents the loss of NeuAc from the sialylated component. The signals at *m/z* 474.2 (reducing end fucosylated HexNAc) and *m/z* 1317.7 $[FucHex_3HexNAc_2]$ are indicative of core fucosylation, while peaks at *m/z* 1021.5 and 2141.2 establish the presence of a sialyl Le^x antennae. Signals at *m/z* 847.4 and 2316.4 confirm that one of the antennae does not carry a fucose. Confirmation of the bi- and/or tri-antennary nature of the non-sialylated constituents (as opposed to a tetra-antennary form of the same composition) comes from ions observed at *m/z* 935.4 and 2230.5, representing loss of a single antenna consisting of $Hex_2HexNAc_2$. LacNAc extensions are also sequentially lost, as demonstrated by signals at *m/z* 2680.3 and 2216.2.

PolyLacNAc containing N-glycans

In order to obtain further structural information on the relative abundance of glycans having the same empirical formula but varying antennae structures, a portion of the underivatised N-glycan mixture was digested with a broad spectrum *Vibrio cholerae* neuraminidase. The resulting sample was permethylated and analysed by MS and MS/MS methods. The MS spectrum of the desialylated N-glycans showed a smaller number of molecular ion signals which were better resolved as compared to the native spectrum because the desialylated sample no longer contained compositions that were closely similar in mass (Fig. 3 and Table 2). We were able to capitalise on the reduced complexity, coupled with the concomitant higher abundance of many of the molecular ions to investigate branching arrangements of the polyLacNAc-containing components. For example, the MS/MS spectrum of the molecular ion $[M+Na]^+$ *m/z* 3765, which has an empirical composition of $Fuc_2Hex_7HexNAc_8$, contained a series of fragment ions carrying information on antennae length, in addition to the most abundant fragment ion (*m/z* 3302.8) which arises from loss of a non-reducing LacNAc (Fig. 4).

The fragment ions *m/z* 2230.3 and 2404.3 confirm the presence of bi-antennary structures with a maximum of three LacNAc units, with and without fucose on the antenna. Signals are observed corresponding to loss of a single Le^x moiety (*m/z* 3127.5) from the non-reducing end of an antenna, as well as signals consistent with the loss of longer portions from a single antenna—Le^x-LacNAc (*m/z* 2678.3) and Le^x-LacNAc-LacNAc (*m/z* 2230.3). Evidence demonstrating the presence of non-fucosylated antennae is present in the form of signals representing the loss from the non-reducing end of a single antenna of one LacNAc (*m/z* 3302.8), two LacNAc's connected in series (*m/z* 2854.2) and three sequential LacNAc structures (*m/z* 2404). Cleavages across multiple antennae are also observed, providing valuable insights into the arrangements of the structural isomers present. The loss of a LacNAc and a Le^x from separate antennae is observed at *m/z* 2664.6, with a related signal showing the loss of a LacNAc from one arm and a Le^x-LacNAc from another seen at *m/z* 2216.3. There are also signals indicating the presence, at low levels, of

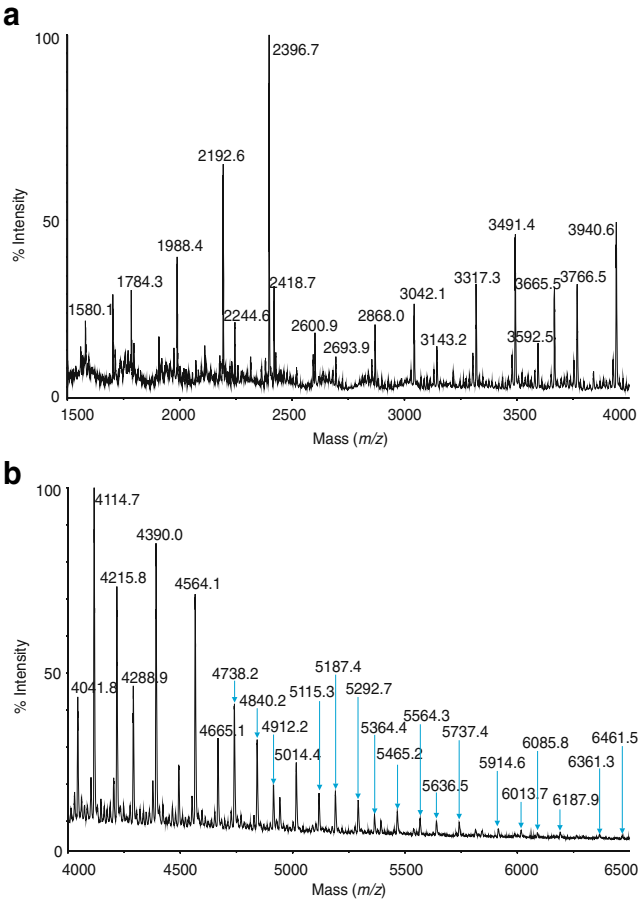

Fig. 3 MALDI-TOF profile of permethylated N-glycans after neuraminidase digestion. Panel (a) shows the lower mass region and panel (b) shows the higher mass region. All molecular ions are present in sodiated form ($[M+Na]^+$)

at least two tri-antennary isomers, with the loss of three separate non-reducing end LacNAc's being observed at *m/z* 2376 and the loss of two LacNAc antennae plus a Le^x antennal epitope seen at *m/z* 2202.3.

MALDI-TOF analysis of released O-glycans from human neutrophils

O-glycans were chemically released by reductive elimination and their permethyl derivatives were analysed by MALDI-TOF MS. The O-glycan profile (Fig. 5 and Table 3) demonstrates that the most abundant glycan species is a fucosylated core-2 glycan (*m/z* 1157.8). There is extensive sialylation among the larger structures present, with disialylated core 1 glycans being observed (*m/z* 1256.8) alongside the more prevalent mono- and di-sialylated core 2 structures (*m/z* 1344.9 and 1706.1). The higher mass regions contain fucosylated signals consistent with Le^x and sialyl Le^x epitopes (*m/z* 2142.4) as well as polyLacNAc extensions (*m/z* 2329.4).

MALDI-TOF/TOF analysis of released O-glycans from human neutrophils

Exemplar data from these experiments are shown in Fig. 6. In similar fashion to the N-glycans, MSMS analysis was consistent across the two geographically remote sample

Table 2 Compositional assignments of singly charged sodiated molecular ions, $[M+Na]^+$, observed in MALDI-MS spectra of permethylated N-glycans after neuraminidase digestion

Signal *m/z*	Molecular Assignments
1580.2	$Hex_5HexNAc_2$
1784.3	$Hex_6HexNAc_2$
1988.4	$Hex_7HexNAc_2$
2192.6	$Hex_8HexNAc_2$
2244.6	$Fuc_1Hex_5HexNAc_4$
2396.7	$Hex_9HexNAc_2$
2418.7	$Fuc_2Hex_5HexNAc_4$
2600.8	$Hex_{10}HexNAc_2$
2693.9	$Fuc_1Hex_6HexNAc_5$
2868.0	$Fuc_2Hex_6HexNAc_5$
3042.1	$Fuc_1Hex_6HexNAc_5$
3143.2	$Fuc_1Hex_7HexNAc_6$
3317.3	$Fuc_2Hex_7HexNAc_6$
3491.4	$Fuc_3Hex_7HexNAc_6$
3592.5	$Fuc_1Hex_8HexNAc_7$
3665.5	$Fuc_4Hex_7HexNAc_6$
3766.6	$Fuc_2Hex_8HexNAc_7$
3940.7	$Fuc_3Hex_8HexNAc_7$
4041.8	$Fuc_1Hex_9HexNAc_8$
4114.8	$Fuc_4Hex_8HexNAc_7$
4215.9	$Fuc_2Hex_9HexNAc_8$
4288.9	$Fuc_5Hex_8HexNAc_7$
4390.0	$Fuc_3Hex_9HexNAc_8$
4491.0	$Fuc_1Hex_{10}HexNAc_9$
4564.1	$Fuc_4Hex_9HexNAc_8$
4665.1	$Fuc_2Hex_{10}HexNAc_9$
4738.2	$Fuc_5Hex_9HexNAc_8$
4840.2	$Fuc_3Hex_{10}HexNAc_9$
4912.2	$Fuc_6Hex_9HexNAc_8$
4940.2	$Fuc_1Hex_{11}HexNAc_{10}$
5014.3	$Fuc_3Hex_{10}HexNAc_9$
5115.3	$Fuc_2Hex_{11}HexNAc_{10}$
5187.4	$Fuc_4Hex_{10}HexNAc_9$
5288.7	$Fuc_3Hex_{11}HexNAc_{10}$
5364.4	$Fuc_5Hex_{10}HexNAc_9$
5465.2	$Fuc_4Hex_{11}HexNAc_{10}$
5564.3	$Fuc_2Hex_{12}HexNAc_{11}$
5636.5	$Fuc_5Hex_{11}HexNAc_{10}$
5737.4	$Fuc_3Hex_{12}HexNAc_{11}$
5914.6	$Fuc_4Hex_{12}HexNAc_{11}$
6013.7	$Fuc_2Hex_{13}HexNAc_{12}$
6085.8	$Fuc_4Hex_{12}HexNAc_{11}$
6187.9	$Fuc_3Hex_{13}HexNAc_{12}$
6361.3	$Fuc_4Hex_{13}HexNAc_{12}$
6461.5	$Fuc_2Hex_{14}HexNAc_{13}$

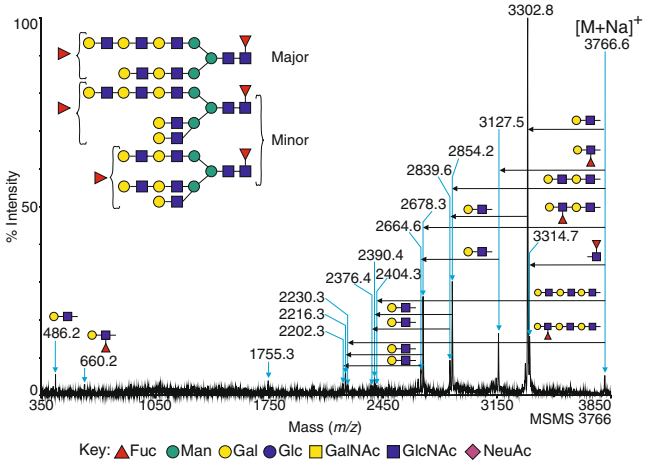

Fig. 4 MALDI-TOF/TOF mass spectrum of the $[M+Na]^+$ molecular ion *m/z* 3765 (composition $Fuc_2Hex_8HexNAc_9$), derived from the neuraminidase treated permethylated N-glycans from neutrophil Sample 2 (UK)

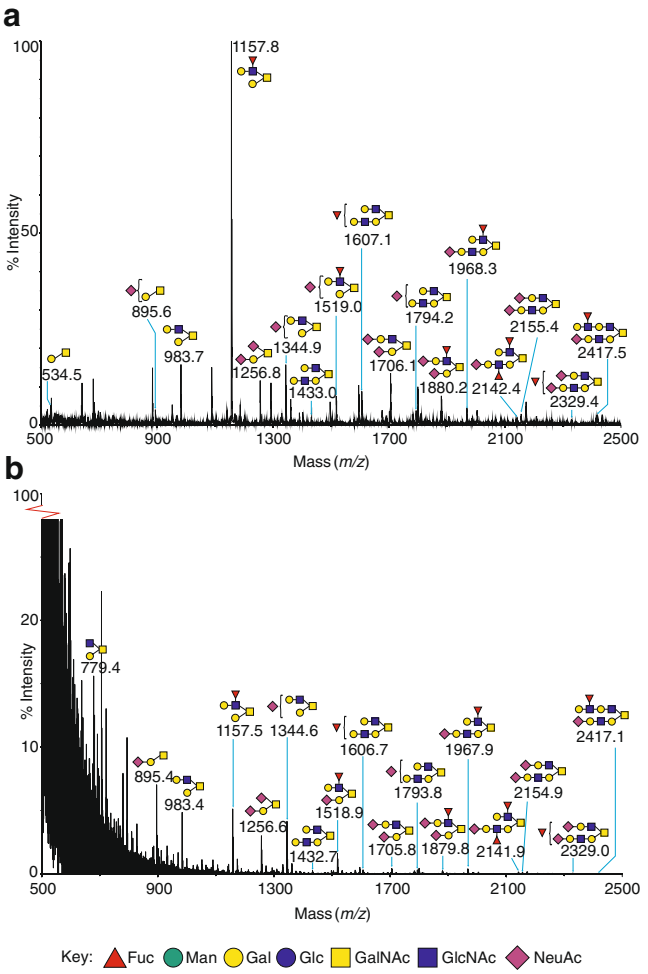

Fig. 5 MALDI-TOF MS profiles of the permethylated O-linked glycans from human neutrophils. Major peaks are annotated with the relevant carbohydrate structure shown in symbol form, according to the glycan nomenclature adopted by the CFG (http://www.functionalglycomics.org/). Neutrophil Sample 1 (US) is displayed in panel a), while neutrophil Sample 2 (UK) is displayed in panel (b)

Table 3 Compositional assignments of singly charged sodiated molecular ions, $[M+Na]^+$, observed in MALDI-MS spectra of permethylated O-glycans from human neutrophils

Signal (*m/z*) Sample 1 (US)	Signal (*m/z*) Sample 2 (UK)	Molecular Assignments
534.5	–	$Hex_1HexNAc_1$-itol
–	779.4	$Hex_1HexNAc_2$-itol
895.6	895.4	$NeuAc_1Hex_1HexNAc_1$-itol
983.7	983.4	$Hex_2HexNAc_2$-itol
1157.8	1157.5	$Fuc_1Hex_2HexNAc_2$-itol
1256.8	1256.6	$NeuAc_2Hex_1HexNAc_1$-itol
1344.9	1344.6	$NeuAc_1Hex_2HexNAc_2$-itol
1433.0	1432.7	$Hex_3HexNAc_3$-itol
1519.0	1518.7	$NeuAc_1Fuc_1Hex_2HexNAc_2$-itol
1607.1	1606.7	$Fuc_1Hex_3HexNAc_3$-itol
1706.1	1705.8	$NeuAc_2Hex_2HexNAc_2$-itol
1794.2	1793.8	$NeuAc_1Hex_3HexNAc_3$-itol
1880.2	1879.8	$NeuAc_2Fuc_1Hex_2HexNAc_2$-itol
1968.3	1967.9	$NeuAc_1Fuc_1Hex_3HexNAc_3$-itol
2142.4	2141.9	$NeuAc_1Fuc_2Hex_3HexNAc_3$-itol
2155.4	2154.9	$NeuAc_2Hex_3HexNAc_3$-itol
2329.4	2329.0	$NeuAc_2Fuc_1Hex_3HexNAc_3$-itol
2417.5	2417.1	$NeuAc_1Fuc_1Hex_4HexNAc_4$-itol

sets. The analysis of the molecular ion at *m/z* 1518.0 demonstrates that this is a core-2 O-glycan and in accord with the N-glycans, sialylation and fucosylation occur on separate antennae. Thus, there is no evidence of a sialyl Le^x containing structural isomer, and instead the NeuAc is located on the 3′-arm of the core-2 structure as shown by fragment ions at *m/z* 620.3 and 921.5, while the fucose residue is present on the 6′-arm of the core-2 in the context of a Le^x structure (*m/z* 472.2, 660.3 and 881.4).

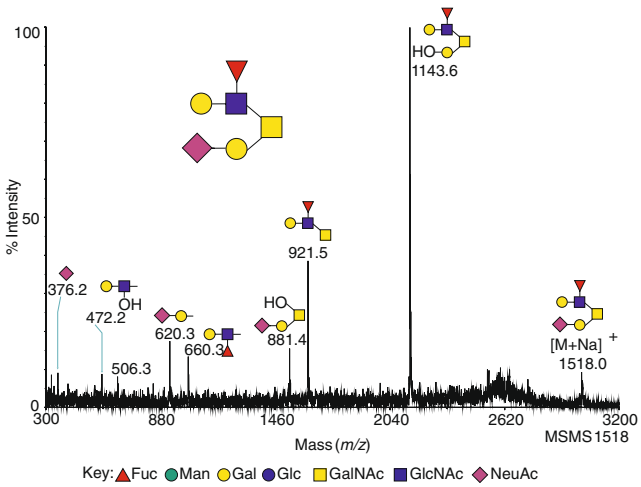

Fig. 6 MALDI-TOF/TOF mass spectrum of the $[M+Na]^+$ molecular ion *m/z* 1518.0 derived from the permethylated O-glycans of neutrophil Sample 2 (UK). Assignments of the fragment ions are labelled

Discussion

The results presented herein on the structural analyses of N- and O-glycans from resting neutrophils exemplify the rapid and very high sensitive detection capabilities of MALDI-TOF/TOF mass spectrometry based glycomics methodology. They clearly demonstrate the mass spectrometric analytical advancements that have been made in upper mass range, resolution, sensitivity and signal to noise ratios in comparison to previous FAB-MS analyses [14]. The initial screening of N-glycans from neutrophils using MALDI-TOF MS revealed the following characteristics; i) high mannose type structures $Man_5GlcNAc_2$ to $Man_9GlcNAc_2$ are present in relatively minor quantities, ii) complex N-glycan structures of mass up to *m/z* 6500 have been observed with the *m/z* 2779 peak being most abundant, iii) the majority of the glycans are core fucosylated, iv) di-, tri- and tetra-antennary structures with polyLacNAc (3Galβ1–4GlcNAc) structures are present, v) an unusually high degree of truncated structures are observed with the signal at *m/z* 2156 being the second most abundant glycan (see Fig. 1). Consistent with earlier work [9] our glycomics study showed that sialyl Le^x, Le^x and polyLacNAc epitopes are terminal groups decorating the N-glycans in neutrophils. The abundance of sialyl Le^x-containing structures was substantially lower compared to the Le^x terminated structures. The glycome profile of the O-glycans consists of both core 1 and core 2 oligosaccharides with sialyl Le^x and Le^x as terminal epitopes. A similar trend is observed for the ratio of sialyl Le^x and Le^x containing structures to that of the N-glycans. In addition, the variation in the data between the two cell preparations was minimal, further reinforcing the findings of the 2007 HUPO study where the MALDI-MS analysis of permethylated N-glycans from transferrin and IgG were shown to be highly sensitive and reproducible [17].

The low abundance of sialyl Le^x containing structures observed in both N- and O-glycans suggests that the availability and display of the active selectin ligands is likely to be restricted to a few glycoproteins on the surface of resting leukocytes. A large body of evidence suggests that both P- and E-selectins bind to distinct sites on P-selectin glycoprotein ligand-1 (PSGL-1), which is a relatively low-abundance glycoprotein on the cell surface [14]. Furthermore, O-glycans mainly contribute to PSGL-1 binding to P-selectins, whereas E-selectin binding has been associated with sialylated fucosyl N-glycans present on E-selectin ligand-1 (ESL-1) [25–28]. Interestingly, only a minor portion of N- and O-glycans in PSGL-1 have been suggested to be involved in selectin binding by radio labelled glycan analysis [29–31]. In addition, sialyl Le^x containing glycans present on PSGL-1 have also been implicated in the aggregation of neutrophils by binding with L-selectins present on the other neutrophils at the inflammation site [32]. These studies demonstrate that preferential binding of selective sialyl Le^x receptors to different selectin molecules has many biological implications.

Careful analyses of the isotopic distribution pattern of each of the peaks present in the entire N-glycan MS spectrum, especially the minor components, showed the presence of more than one instance of overlapping of signals. For example, the peak *m/z* 3141 consists of two glycans of *m/z* 3141 and 3143 in a ratio of approximately 1:1 (Fig. 2b). The collision activated decomposition (CAD) MS/MS analysis of this peak revealed that indeed the presence of sialyl Le^x containing core fucosylated bi-antennary glycan (*m/z* 3141.0) and a mixture of LacNAc terminated bi- and tri-antennary glycans (*m/z* 3143.0). The exoglycosidase assay also supported the finding by MS/MS analysis, in which the peak *m/z* 3141.0 disappeared but not *m/z* 3143.0 after treatment with broad spectrum neuraminidase. More interestingly, the percentage abundance of this peak in whole of the neutrophil N-glycans is about 0.008%. These results profoundly demonstrated the power and very high sensitivity of glycomics methodology based on mass spectrometric analysis.

After neuraminidase treatment the N-glycan signals become more spread out facilitating MS/MS analyses of glycans up *m/z* 6000. This enzymatic degradation allowed us to readily explore the branching patterns of mixtures of isobaric glycans by tandem mass spectrometry. For example, TOF/TOF analysis of the permethylated glycan of mass *m/z* 3766 showed that it mainly consists of more than one isoform of a bi-antennary glycan with terminal polyLacNAc and Le^x structures (Fig. 4). No significant levels of tri- or tetra-antennary structures were observed in this peak. These studies involving enzymology and mass spectral data analysis again demonstrate that the current glycomics methodology can very effectively be used to obtain detailed structural information about specific complex glycans from within a large pool closely related structures.

The polyLacNAc glycans of the types that we have observed on neutrophils have been shown to bind to a variety of galectins [33–35]. However, binding of galectin-1 and galectin-3 with neutrophil polyLacNAc ligands exhibit contrasting functions. For example, the galectin-1 binding inhibits chemotaxis and extravasation where as the galectin-3 enhances both of these functions [36–38]. In addition, galectin-1 and galectin-3 induce phosphatidylserine exposure in human neutrophils without apoptosis, but galectin-3, but not galectin-1, induces apoptosis of activated T cells [39]. Diversity of sialylated fucosyl polyLacNAc glycans present on the neutrophils supports the hypothesis that different glycans bind to different glycan receptors leading to manifestation of fundamentally different biological functions [33].

Acknowledgements Ponnusamy Babu was supported by a UK-India Education and Research Initiative (UKIERI) research fellowship. The glycan analyses were performed by the Analytical Glycotechnology Core of the Consortium for Functional Glycomics (GM62116). Anne Dell was a Biotechnology and Biological Sciences Research Council (BBSRC) Professorial Fellow. RDC was supported by National Institutes of Health (NIH) Grant *RO1AI48075*. SMR *was supported by a grant from the European Community* Innovative Chemokine-based Therapeutic Strategies for Autoimmunity and Chronic Inflammation *(INNOCHEM), the Wellcome Trust and the British Heart Foundation*. The authors thank Annette Fleshman and Dr. Ziad Kawar for their assistance.

References

1. Crowther, D.J.: Applications of microarrays in the pharmaceutical industry. Curr. Opin. Pharmacol. **2**, 551–554 (2002)
2. Zarbock, A., Ley, K.: Mechanisms and consequences of neutrophil interaction with the endothelium. Am. J. Pathol. **172**, 1–7 (2008)
3. McEver, R.P.: Adhesive interactions of leukocytes, platelets, and the vessel wall during hemostasis and inflammation. Thromb. Haemost. **86**, 746–756 (2001)
4. Lekstrom-Himes, J.A., Gallin, J.I.: Immunodeficiency diseases caused by defects in phagocytes. N. Engl. J. Med. **343**, 1703–1714 (2000)
5. Rotrosen, D., Gallin, J.I.: Disorders of phagocyte function. Annu. Rev. Immunol. **5**, 127–150 (1987)
6. Etzioni, A., Frydman, M., Pollack, S., Avidor, I., Phillips, M.L., Paulson, J.C., Gershoni-Baruch, R.: Brief report: recurrent severe infections caused by a novel leukocyte adhesion deficiency. N. Engl. J. Med. **327**, 1789–1792 (1992)
7. Etzioni, A.: Leukocyte adhesion deficiencies: molecular basis, clinical findings, and therapeutic options. Adv. Exp. Med. Biol. **601**, 51–60 (2007)
8. Lowe, J.B.: Glycosylation in the control of selectin counter-receptor structure and function. Immunol. Rev. **186**, 19–36 (2002)
9. Fukuda, M., Spooncer, E., Oates, J.E., Dell, A., Klock, J.C.: Structure of sialylated fucosyl lactosaminoglycan isolated from human granulocytes. J. Biol. Chem. **259**, 10925–10935 (1984)
10. Drickamer, K.: Two distinct classes of carbohydrate-recognition domains in animal lectins. J. Biol. Chem. **263**, 9557–9560 (1988)
11. Weis, W.I., Taylor, M.E., Drickamer, K.: The C-type lectin superfamily in the immune system. Immunol. Rev. **163**, 19–34 (1998)
12. Rosen, S.D.: Ligands for L-selectin: homing, inflammation, and beyond. Annu. Rev. Immunol. **22**, 129–156 (2004)
13. Rosen, S.D., Bertozzi, C.R.: The selectins and their ligands. Curr. Opin. Cell. Biol. **6**, 663–673 (1994)
14. McEver, R.P., Cummings, R.D.: Role of PSGL-1 binding to selectins in leukocyte recruitment. J. Clin. Invest. **100**, S97–103 (1997)
15. Dell, A.: F.A.B.-mass spectrometry of carbohydrates. Adv. Carbohydr. Chem. Biochem. **45**, 19–72 (1987)
16. Haslam, S.M., North, S.J., Dell, A.: Mass spectrometric analysis of N- and O-glycosylation of tissues and cells. Curr. Opin. Struct. Biol. **16**, 584–591 (2006)
17. Wada, Y., Azadi, P., Costello, C.E., Dell, A., Dwek, R.A., Geyer, H., Geyer, R., Kakehi, K., Karlsson, N.G., Kato, K., Kawasaki, N., Khoo, K.H., Kim, S., Kondo, A., Lattova, E., Mechref, Y., Miyoshi, E., Nakamura, K., Narimatsu, H., Novotny, M.V., Packer, N.H., Perreault, H., Peter-Katalinic, J., Pohlentz, G., Reinhold, V.N., Rudd, P.M., Suzuki, A., Taniguchi, N.: Comparison of the methods for profiling glycoprotein glycans—HUPO Human Disease Glycomics/Proteome Initiative multi-institutional study. Glycobiology **17**, 411–422 (2007)
18. Zimmerman, G.A., McIntyre, T.M., Prescott, S.M.: Thrombin stimulates the adherence of neutrophils to human endothelial cells in vitro. J. Clin. Invest. **76**, 2235–2246 (1985)
19. Haslett, C., Guthrie, L.A., Kopaniak, M.M., Johnston Jr., R.B., Henson, P.M.: Modulation of multiple neutrophil functions by preparative methods or trace concentrations of bacterial lipopolysaccharide. Am. J. Pathol. **119**, 101–110 (1985)
20. Sutton-Smith, M., Dell, A.: Analysis of carbohydrates/glycoproteins by mass spectrometry. In: Celis, J.E. (ed.) Cell Biology: A Laboratory Handbook, pp. 425–435. Academic Press, San Diego, CA (2006)
21. Dell, A., Reason, A.J., Khoo, K.H., Panico, M., McDowell, R.A., Morris, H.R.: Mass spectrometry of carbohydrate-containing biopolymers. Methods Enzymol. **230**, 108–132 (1994)
22. Dell, A., Khoo, K.H., Panico, M., McDowell, R.A., Etienne, A.T., Reason, A.J., Morris, H.R.: FAB-MS and ES-MS of glycoproteins. In: Fukuda, M., Kobata, A. (eds.) Glycobiology: A Practical Approach, pp. 187–222. Oxford University Press, Oxford (1993)
23. Goldberg, D., Sutton-Smith, M., Paulson, J., Dell, A.: Automatic annotation of matrix-assisted laser desorption/ionization N-glycan spectra. Proteomics **5**, 865–875 (2005)
24. Ceroni, A., Maass, K., Geyer, H., Geyer, R., Dell, A., Haslam, S. M: GlycoWorkbench: A tool for the computer-assisted annotation of mass spectra of glycans. J. Proteome. Res. **7**, 1650–1659 (2008)
25. Patel, T.P., Goelz, S.E., Lobb, R.R., Parekh, R.B.: Isolation and characterization of natural protein-associated carbohydrate ligands for E-selectin. Biochemistry **33**, 14815–14824 (1994)
26. Vestweber, D.: Ligand-specificity of the selectins. J. Cell. Biochem. **61**, 585–591 (1996)
27. Hidalgo, A., Peired, A.J., Wild, M.K., Vestweber, D., Frenette, P.S.: Complete identification of E-selectin ligands on neutrophils reveals distinct functions of PSGL-1, ESL-1, and CD44. Immunity **26**, 477–489 (2007)
28. Lenter, M., Levinovitz, A., Isenmann, S., Vestweber, D.: Monospecific and common glycoprotein ligands for E- and P-selectin on myeloid cells. J. Cell Biol. **125**, 471–481 (1994)
29. Aeed, P.A., Geng, J.G., Asa, D., Raycroft, L., Ma, L., Elhammer, A.P.: Characterization of the O-linked oligosaccharide structures on P-selectin glycoprotein ligand-1 (PSGL-1). Glycoconj. J. **15**, 975–985 (1998)
30. Aeed, P.A., Geng, J.G., Asa, D., Raycroft, L., Ma, L., Elhammer, A.P.: Partial characterization of the N-linked oligosaccharide structures on P-selectin glycoprotein ligand-1 (PSGL-1). Cell Res. **11**, 28–36 (2001)
31. Wilkins, P.P., McEver, R.P., Cummings, R.D.: Structures of the O-glycans on P-selectin glycoprotein ligand-1 from HL-60 cells. J. Biol. Chem. **271**, 18732–18742 (1996)
32. Guyer, D.A., Moore, K.L., Lynam, E.B., Schammel, C.M., Rogelj, S., McEver, R.P., Sklar, L.A.: P-selectin glycoprotein ligand-1 (PSGL-1) is a ligand for L-selectin in neutrophil aggregation. Blood **88**, 2415–2421 (1996)
33. Stowell, S.R., Arthur, C.M., Mehta, P., Slanina, K.A., Blixt, O., Leffler, H., Smith, D.F., Cummings, R.D.: Galectins-1, -2 and -3 exhibit differential recognition of sialylated glycans and blood group antigens. J. Biol. Chem. **283**, 10109–10123 (2008)
34. Patnaik, S.K., Potvin, B., Carlsson, S., Sturm, D., Leffler, H., Stanley, P.: Complex N-glycans are the major ligands for galectin-1, -3, and -8 on Chinese hamster ovary cells. Glycobiology **16**, 305–317 (2006)

35. Leppanen, A., Stowell, S., Blixt, O., Cummings, R.D.: Dimeric galectin-1 binds with high affinity to alpha2,3-sialylated and non-sialylated terminal N-acetyllactosamine units on surface-bound extended glycans. J. Biol. Chem. **280**, 5549–5562 (2005)
36. La, M., Cao, T.V., Cerchiaro, G., Chilton, K., Hirabayashi, J., Kasai, K., Oliani, S.M., Chernajovsky, Y., Perretti, M.: A novel biological activity for galectin-1: inhibition of leukocyte-endothelial cell interactions in experimental inflammation. Am. J. Pathol. **163**, 1505–1515 (2003)
37. Sano, H., Hsu, D.K., Yu, L., Apgar, J.R., Kuwabara, I., Yamanaka, T., Hirashima, M., Liu, F.T.: Human galectin-3 is a novel chemoattractant for monocytes and macrophages. J. Immunol. **165**, 2156–2164 (2000)
38. Hsu, D.K., Yang, R.Y., Pan, Z., Yu, L., Salomon, D.R., Fung-Leung, W.P., Liu, F.T.: Targeted disruption of the galectin-3 gene results in attenuated peritoneal inflammatory responses. Am. J. Pathol. **156**, 1073–1083 (2000)
39. Stowell, S.R., Qian, Y., Karmakar, S., Koyama, N.S., Dias-Baruffi, M., Leffler, H., McEver, R.P., Cummings, R.D.: Differential roles of galectin-1 and galectin-3 in regulating leukocyte viability and cytokine secretion. J. Immunol. **180**, 3091–3102 (2008)